Search for a torsion field in $pp \to e^+e^- + X$ collisions at $\sqrt{s} = 8$ TeV with the ATLAS/LHC

Simão Paulo Silva

Summer School and Workshop on High Energy Physics at the LHC: New trends in HEP and QCD

November 5, 2014

Introduction

Actually, the best theory that describes the elementary particles and their interactions is the Standard Model (SM), due to its great agreement with the experimental data, that includes the experimental discovery of the Higgs boson at LHC.

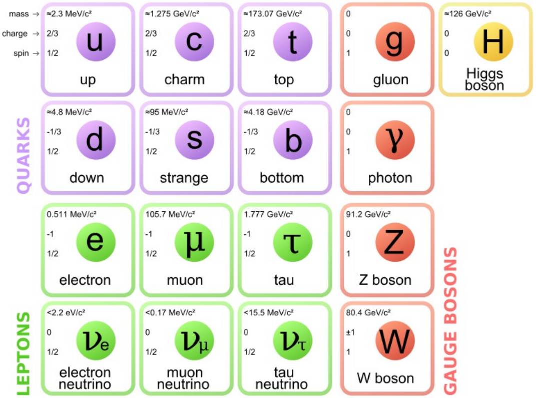

Despite the good agreement with the available experimental data, the SM also has its limitations.

For example, gravity is not included in SM yet, the dark matter cannot be described in terms of the SM particles, the SM cannot explain why there are exactly three generations of particles or if the elementary particles can be composed of other unknown particles.

Such questions lead to the development of new models and SM extensions. Many of these models contain new particles and interactions, like the graviton, SUSY partners, Z' and/or W', and many others.

A field predicted in many extensions of General Relativity is the torsion field, described in next section.

The goal of this work is the search for a torsion field using the data collected by the ATLAS detector in 2012, in $pp \to e^+e^- + X$ channel, with $\sqrt{s} = 8$ TeV and an integrated luminosity of $\int Ldt = 20.3$ fb^{-1}.

The analysis methods used in this work were the same used by the specific group of the ATLAS collaboration assigned to search for other high mass resonances, like Z'[1].

[1] ATLAS Collaboration, Phys. Rev. D 90, 052005, 2014

The torsion field
Classical definition

The covariant derivative of a contravariant vector A^μ can be written as

$$\nabla_\beta A^\alpha = \partial_\beta A^\alpha + \Gamma^\alpha{}_{\beta\gamma} A^\gamma, \tag{1}$$

where $\Gamma^\alpha{}_{\beta\gamma}$ is a connection with transformation properties different from those of a tensor. If $\Gamma^\alpha{}_{\beta\gamma}$ satisfies the symmetry condition, $\Gamma^\alpha{}_{\beta\gamma} = \Gamma^\alpha{}_{\gamma\beta}$, and the metricity condition $\nabla_\alpha g_{\mu\nu} = 0$, $\Gamma^\alpha{}_{\beta\gamma}$ is the so called Christoffel symbol of second kind. One can choose a connection $\tilde{\Gamma}^\alpha{}_{\beta\gamma}$ that satisfies the metricity condition, but is antisymmetric, so a new tensor called torsion can be defined as

$$T^\alpha{}_{\beta\gamma} = \tilde{\Gamma}^\alpha{}_{\beta\gamma} - \tilde{\Gamma}^\alpha{}_{\gamma\beta}. \tag{2}$$

The torsion field can be decomposed in three irreducible components:

$$T_{\alpha\beta\gamma} = \frac{1}{3}\left(T_\beta g_{\alpha\gamma} - T_\gamma g_{\alpha\beta}\right) - \frac{1}{6}\epsilon_{\alpha\beta\gamma\nu}S^\nu + q_{\alpha\beta\gamma}, \qquad (3)$$

where $T_\beta = T^\alpha{}_{\beta\alpha}$ is the vector trace, $S^\nu = \epsilon^{\alpha\beta\gamma\nu}T_{\alpha\beta\gamma}$ is an axial vector, and $q_{\alpha\beta\gamma}$ is a tensor that satifies $q^\alpha{}_{\beta\alpha} = 0$ and $\epsilon^{\alpha\beta\gamma\nu}q_{\alpha\beta\gamma} = 0$.

Torsion-fermion interaction

The action of a fermion interacting with the torsion field, can be written as:

$$S = \int d^4x \left[i\bar{\psi}\gamma^\mu \left(\partial_\mu + \frac{i}{8}\gamma_5 \; S_\mu \right) \psi + m\bar{\psi}\psi \right]. \tag{4}$$

The action above is called minimum action, and the fermion is coupled only in the pseudovector S^μ. Introducing a non-minimal action, we have:

$$S = \int d^4x \left[i\bar{\psi}\gamma^\mu \left(\partial_\mu + i\eta\gamma_5 S_\mu + i\hat{\eta}T_\mu \right) \psi + m\bar{\psi}\psi \right]. \tag{5}$$

Here η and $\hat{\eta}$ are coupling constants. The interaction with the vector T_μ has the same form that the interaction with a electromagnetic field A_μ, then T_μ can be suppressed with a simple redefinition of $A\mu$ in the presence of an electromagnetic field.

$$S = \int d^4x \left[i\bar{\psi}\gamma^\mu \left(\partial_\mu + i\eta\gamma_5 S_\mu + ieA_\mu \right) \psi + m\bar{\psi}\psi \right]. \tag{6}$$

The propagating torsion

Based on symmetry arguments, one can get the following form of the propagating torsion action:

$$S_{tor} = \int d^4x \left[-aS_{\mu\nu}S^{\mu\nu} + b(\partial_\mu S^\mu)^2 + M_{TS}^2 S_\mu S^\mu\right], \tag{7}$$

where M_{TS} is the torsion mass, a and b are constants and $S_{\mu\nu} = \partial_\mu S_\nu - \partial_\nu S_\mu$. Due to the requirement that the symmetries are conserved in renormalization and the theory is unitary, $b = 0$ and only the vectorial mode propagates. By convention, choosing $a = 1/4$:

$$S_{tor} = \int d^4x \left[-\frac{1}{4}S_{\mu\nu}S^{\mu\nu} + M_{TS}^2 S_\mu S^\mu\right]. \tag{8}$$

η can be different for each fermion and M_{TS} must satisfy $M_{TS} \gg \eta_{fermion} m_{fermion}$. Here we have assumed $\eta_{fermion}$ has the same value $\eta = \eta_{TS}$ for all fermions, and $\hat{\eta} = 0$.

Phenomenology and experimental results

The hard process from $pp \to e^+e^- + X$ collisions interesting for this work is

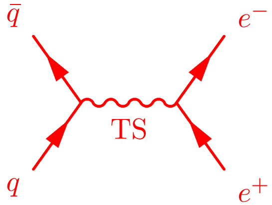

Generally, q is a valence quark and $\bar{q}$ is a sea quark. The major contributions to the cross section are due to $u\bar{u}$ and $d\bar{d}$.

Exclusion graph obtained from simulation of $pp \to e^+e^- + X$ collisions with $\sqrt{s} = 14$ TeV and $\int Ldt = 100$ fb^{-1}.

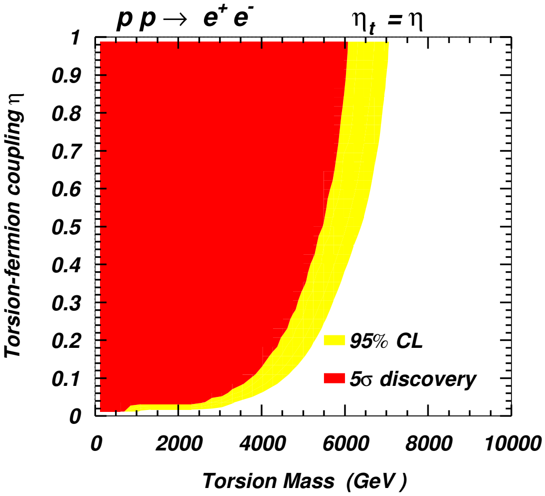

It was showed that for $\eta_{TS} = 0.1$, it is possible to exclude M_{TS} up to 4.5 TeV and, for $\eta_{TS} = 0.5$ more than 6.5 TeV[2].

[2] BELYAEV, A., SHAPIRO, I. VALE, M., Phys. Rev. D, 3 (2007) 75

The first limits of torsion parameter space were based on data collected by TEVATRON and LEP1.5, using $e^+e^- \to l^+l^- + X$ collisions, where l means e or μ. Since there was not enough energy to produce a resonance, the forward-backward asymmetry was used to look for evidences of the torsion field[3].

Limits obtained using $pp \to l^+l^- + X$, with $\sqrt{s} = 7$ TeV and $\int Ldt = 4.9$ fb^{-1} for $e^\pm$ and $\int Ldt = 5.0$ fb^{-1} for $\mu^\pm$, recently published by the ATLAS Collaboration[4].

η	0.05	0.1	0.2	0.3	0.4	0.5
Observed limit [TeV]	1.52	1.94	2.29	2.50	2.69	2.91
Expected limit [TeV]	1.58	1.96	2.31	2.55	2.77	3.02

[3] Belyaev, A., Shapiro I., Nuclear Physics B, 1 (1999) 543

[4] ATLAS Collaboration, JHEP 11 (2012) 138, arXiv:1209.2535v2[hep-ex].

The experimental apparatus

The Large Hadron Collider (LHC)

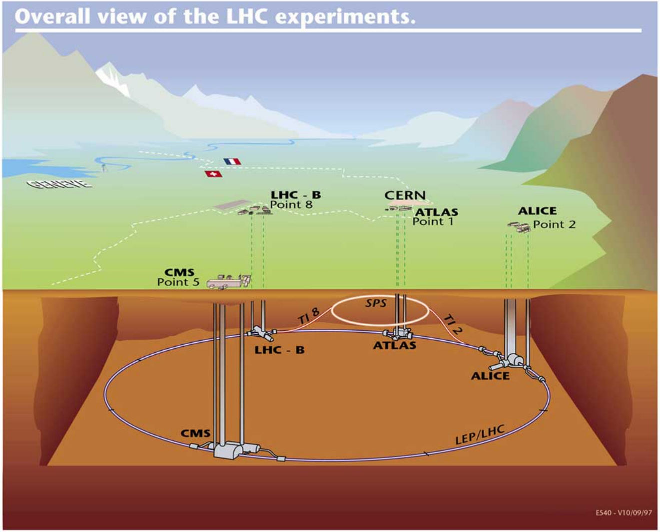

The LHC injection complex

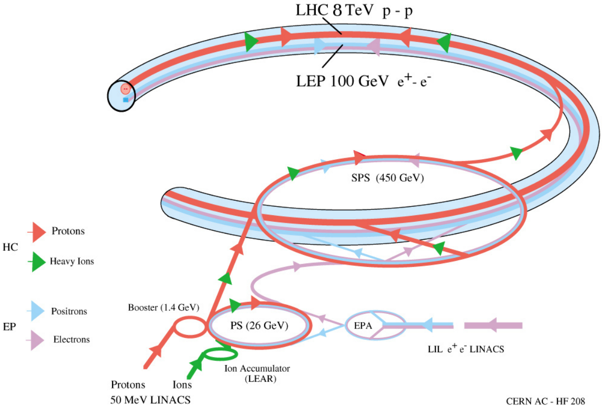

The ATLAS detector

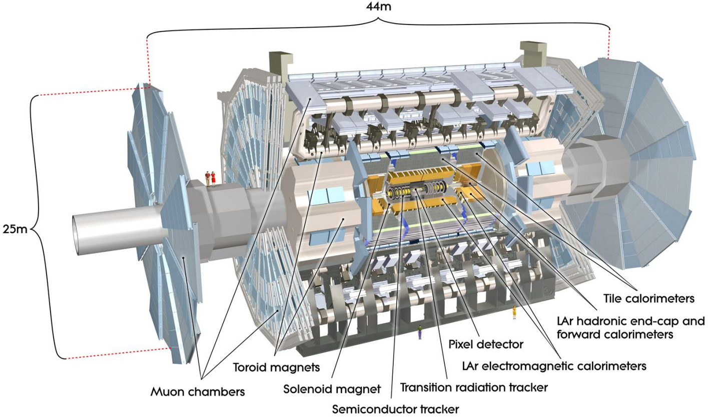

The ATLAS coordinate system and useful definitions

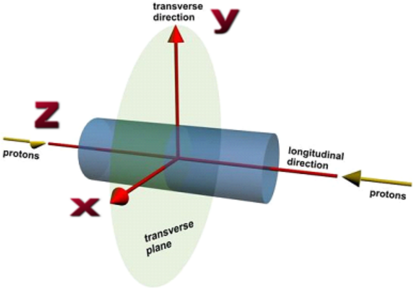

The z axis is the beam axis, the x axis points to the LHC center and the y points to the surface.

If ϕ is the azimutal angle and θ the polar angle, the pseudo-rapidity is defined by $\eta = -\ln\tan\theta/2$. One can define a "radius" on the $\eta\times\phi$ plane as $\Delta R = \sqrt{\Delta\eta^2 + \Delta\phi^2}$. The transverse momentum p_T is the projection of the linear momentum onto the xy plane. The transverse energy is given by $E_T = \sqrt{M^2 + p_T^2}$.

Trigger

In 2012, the time spacing between two collisions was about 50 ns, that leads to a great number of (pile-up) interactions. So, it requires a very efficient filtering system (trigger). The ATLAS trigger system has three levels.

- The first level (L1) is hardware based and reduces the rate of events from 40 MHz to 75 kHz. μs.
- The second level (L2) has an output rate of 2 kHz. It is a software trigger and its analysis is based on regions of interest defined by L1.
- At the final stage, the Event Filter is similar to L2, but it uses offline reconstruction algorithms. Its output rate is 200 Hz.

Data analysis and results

Data samples collected by ATLAS

The experimental data was recorded in 2012, from April to December, from $pp \to e^+e^- + X$ collisions at $\sqrt{s} = 8$ TeV and $\int L dt = 20.3$ fb^{-1}.

- The events passed by a trigger that requires two clusters in the Electromagnetic Calorimeter, with a p_T threshold of 35 GeV for the electron candidate with the highest p_T (leading electron) and 25 GeV for the electron candidate with the second highest p_T (subleading electron).
- Electron candidates must have a well defined track satisfying a set of requirements in order to keep performance at high pile-up conditions[5].
- In order to avoid photon backgrounds, it is required the first layer of the Pixel Detector was hit if an active layer was hit.

[5] The ATLAS Collaboration, The European Physical Journal C, 3 (2012)

72

Backgrounds

All simulated backgrounds passed by the complete simulation of the ATLAS detector, based on the software Geant4, and the final state radiation was handled by Photos. The simulated backgrounds were

- Drell-Yan (DY) is the predominant background, simulated using Powheg and Pythia8, with the CT10 PDF at NLO.
- Backgrounds of processes containing a pair $t\bar{t}$, $\sigma_{t\bar{t}} = 253$ pb, or a top quark associated to a $W^{\pm}$ boson, $\sigma_{Wt} = 22.4$ pb. Events of these kinds were generated by MC@NLO and Herwig with the CT10 PDF.
- The backgrounds involving boson pairs, ZZ, $\sigma_{ZZ} = 7.4$ pb, WZ, $\sigma_{WZ} = 21$ pb, and $W^{+}W^{-}$, $\sigma_{WW} = 57$ pb, were simulated by Herwig with the CTEQ6L1 PDF.

Both the top quark and dibosons backgrounds have low cross sections and were extrapolated to high mass regions.

The jets Backgrounds

The second most important background is is based on jet pairs or jets associated with $W^{\pm}$ bosons. These backgrounds were estimated using a data-driven method, since it is too dificulty to simulate jets misidentified as electrons.

The probability of a jet is misidentified as an electron was estimated based on the fraction of leading or subleading electron candidates that passed several trigger conditions in the range of transverse energy 25 GeV$< E_T <$360 GeV. The remained candidates were submited to a more rigid set of tests. The fake rate is about 10%.

Drell-Yan simulated samples

The e^+e^- invariant mass M_{ee} histograms (templates) were obtained from Drell-Yan M_{ee} histograms by applying weights. The application of weights allows us to get templates for several masses and coupling constants without performing the complete detector simulation many times.

The DY samples used for weighting were generated by Pythia8 with the MSTW2008LO PDF. These events passed by the complete simulation of the ATLAS detector and the FSR was handled by Photos.

Event selection

The main selection criteria were:

- Events that passed the photon thrigger.
- Events must have at least two electrons.
- Events must have at least one vertex with three tracks.
- At least two electrons must have $p_T > 30$ GeV.
- The pseudo-rapidity must be within $|\eta| < 2.47$, but must not be in $1.37 < |\eta| < 1.52$.
- At least one electron must have $p_T > 40$ GeV.
- The electron pair invariant mass must be greater than 80 GeV.

It was not required opposite charges because of the possibility of charge misidentification, due to bremsstrahlung or low track deflection.

Signal templates simulation

It was created M_{ee} histograms from 128 GeV to 4500 GeV. The bin width is constant in $\log M_{ee}$.
Signal templates were generated by applying the weight function $\mathcal{W}(m_{ee}, q)$, whose arguments are the dielectron pair invariant mass m_{ee} before the detector simulation and the incident quark flavor q.

$$\mathcal{W}(m_{ee}, q) = \frac{|TS|}{|DY|}, \qquad (9)$$

TS and DY are the helicity amplitudes of the torsion and Drell-Yan, respectively. It was generated templates for torsion masses from 150 GeV to 4000 GeV, with 50 GeV increments. The coupling constants used were η_{TS}=0.05, 0.1, 0.2, 0.3, 0.4 and 0.5.
Weights were also applied to include corrections on reconstruction and idenfification efficiencies, correct the pileup conditions and estimate the cross section at NNLO (k-factor).

Data, backgrounds and templates comparison

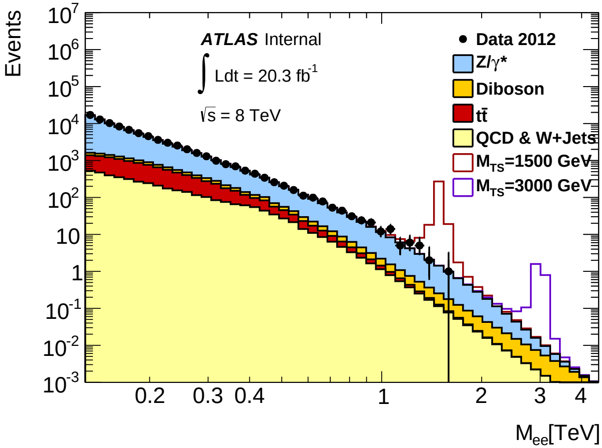

It was assumed $\eta_{TS} = 0.2$ for the templates showed in the figure above.

Acceptance times efficiency ($A \times \epsilon$)

The acceptance times efficiency $A \times \epsilon$ is the ratio between the number of simulated survivor events (that passed the detector simulations and the event selection) in the M_{ee} interval of the search region and the total number of events in the same mass range.

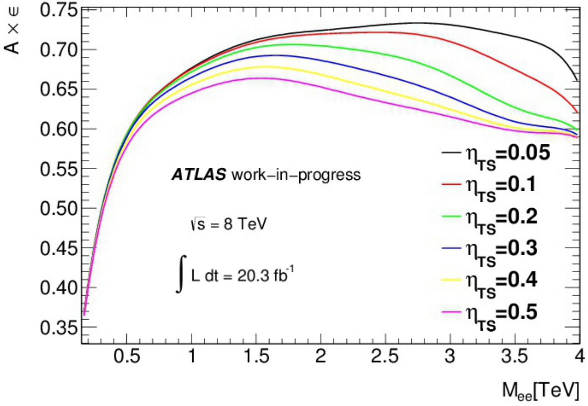

Statistical analysis

The likelihood function for a M_{ee} histogram of N_{bin} bins is

$$\mathcal{L}(data|N_j,\nu_i) = \prod_{k=1}^{N_{bin}} \frac{\mu_k^{n_k} e^{-\mu_k}}{n_k!} \prod_{i=1}^{N_{sys}} G(\nu_i), \qquad (10)$$

where $G(\nu_i)$ is a probability density function of the nuisance parameter ν_i, $\mu_k = N_{signal} + N_{backgrounds}$ events of the bin k and n_k is the number of events observed in this bin.

The likelihood function can be reduced to a function of one parameter of interest integrating over the nuisance parameters.

$$\mathcal{L}'(data|N_{TS}) = \int \mathcal{L}(N_j,\vec{\nu})d\vec{\nu}. \qquad (11)$$

The reduced likelihood is converted into a posterior probability density using the Baye's theorem.

The parameter of interest was chosen to be the product cross section times branching-ratio σB.

The 95% Bayesian upper limit $(\sigma B)_{95}$ is obtained by solving

$$0,95 = \frac{\int_0^{(\sigma B)_{95}} \mathcal{L}'(\sigma B|data)\pi(\sigma B)d(\sigma B)}{\int_0^{\infty} \mathcal{L}'(\sigma B|data)\pi(\sigma B)d(\sigma B)}. \tag{12}$$

The expected limits were calculated using 200 pseudo-experiments with only SM processes. The median of each distribution was chosen to be the expected limit.

The σB limits can be converted in torsion mass limits using plots $(\sigma B)_{95} \times M_{TS}$. The expected and observed mass limits are the intersection of the theoretical curves with the expected and observed $(\sigma B)_{95}$, respectively.

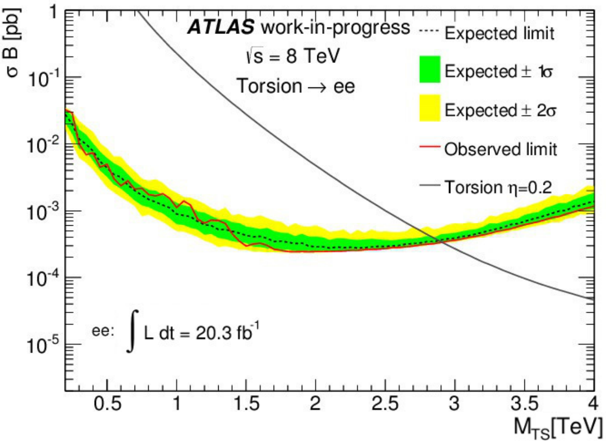

Expected and observed limits for $\eta_{TS} = 0.2$, showing the 68% e 95% contours.

Systematic uncertainties

The systematic uncertainties were incorporated as nuisance parameters in the likelihood function.

The most relevant theoretical uncertainties were the MSTW2008 PDF error and the PDF choice uncertainty, used in the Drell-Yan background simulation.

The main experimental source of systematic uncertainties was the determination of the dijets and W+jets backgrounds, that was in overall 20%.

Other uncertainties were less than 3% and were all ignored.

Results

Expected and observed torsion mass limits at $\sqrt{s} = 8$ Tev and $\int Ldt = 20.3$ fb^{-1}.

η_{TS}	0.05	0.1	0.2	0.3	0.4	0.5
Observed limits [TeV]	2.059	2.464	2.906	3.228	3.574	3.989
Expected limits [TeV]	2.045	2.454	2.882	3.171	3.496	3.875

Exclusion graph at 95% CL for the torsion parameter space.

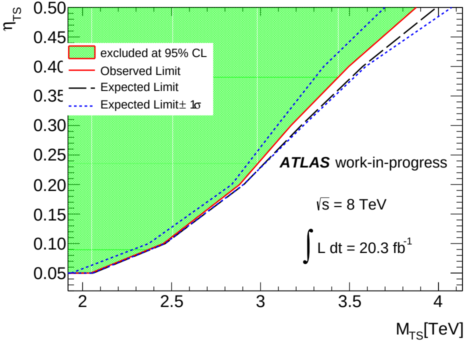

Thank you for your attention!